ULTRAVIOLET DETECTORS

The detection of ultraviolet (UV) radiation is of importance in many applications in science, industry, and medicine, such as flame and spark detection, communications, UV dosimetry of industrial processes such as UV-initiated photopolymerization reactions, and sterilization of equipment and water. The UV light spectrum is generally considered to comprise wavelengths from 10 nm to 400 nm. These wavelengths are traditionally subdivided into several ranges, given in Table 1. Photodetection of ultraviolet light within these ranges poses specific challenges in terms of the fabrication and engineering of photodetector devices and the development of appropriate materials. An excellent review (1) of all types of photodetectors, including ultraviolet-sensitive photodetectors, has been published recently. A detailed review (2) of ultraviolet- and X-ray-sensitive detectors that addresses both imaging and

J. Webster (ed.), *Wiley Encyclopedia of Electrical and Electronics Engineering*. Copyright © 1999 John Wiley & Sons, Inc.

Table 1. Ultraviolet Light Nomenclature

UV Region	Wavelength Range (nm)
Near UV	400–300
Mid UV	300–200
Far UV	200–100
Extreme UV	100–10
UVA	400–320
UVB	320–280
UVC	280–100
Deep UV	350–190
Actinic UV	315–200
Vacuum UV	200–10

nonimaging systems has also been recently published. This article discusses the current commercially available technologies for nonimaging UV photodetection applications. In addition, in view of the fact that UV photodetection is an active and important field of research, emerging technologies are also briefly discussed. The article is divided into two sections, the first addressing UV detection with semiconductor photodiodes and the second covering UV detection with photoemissive phototubes.

SEMICONDUCTOR ULTRAVIOLET PHOTODETECTORS

Semiconductor detectors, used in either the photoconductive or photovoltaic modes, are widely used photoelectric detectors of ultraviolet light. Razeghi and Rogalski (3) have recently published a comprehensive review of ultraviolet-sensitive semiconductor detectors that describes in detail the theory and operation of each different type of detector. Semiconductor detectors are attractive due to their small size, simple operation, and relative low cost, and, for many applications, provide stable, linear detection of ultraviolet light over a wide dynamic range of incident powers. Silicon traditionally has been the most widely used semiconductor material for the fabrication of ultraviolet-sensitive photodetectors; however, its use is limited by radiation-induced aging effects, problems arising from the strong absorption of UV light, and an inability to operate at elevated temperatures. Si photodetectors are also much more sensitive to visible and near-IR light than to UV light. However, silicon wafer processing technology is quite advanced and Si photodetectors have been engineered with features designed to enhance the ultraviolet light sensitivity. The most widely used UV enhanced device structures are junction photodetectors, including, for example, shallow diffused *p–n* junctions and Schottky barriers. In this section we will discuss the characteristics and relative merits of shallow diffused *p–n* junction and Schottky barrier photodiodes, fabricated using a number of materials, including silicon and several wider-band-gap materials such as silicon carbide (SiC), III–V nitrides (GaN, AlGaN) and III–V phosphides (GaAsP, GaP). Wide-band-gap materials are better suited in many ways than Si for UV photodetection. For example, wide-band-gap photodetectors exhibit improved radiation hardness, better resistance to temperature and harsh chemicals, and improved wavelength selectivity (visible blind operation). Consequently, the development of wide-band-gap materials and their application in photodetection is an active area of research.

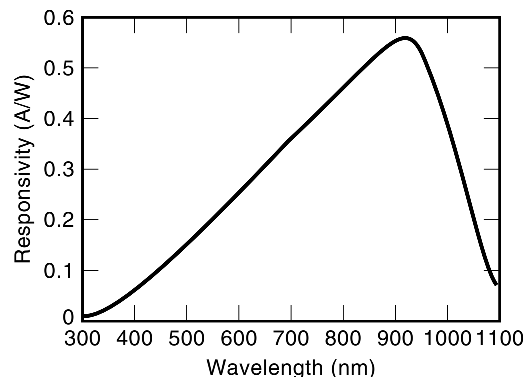

Figure 1. Spectral response of a standard *p–n* junction Si photodiode.

Silicon *p–n* Junction Photodiode

Photodiodes fabricated using *p–n* junctions in silicon have been the most widely used photovoltaic detectors for ultraviolet photodetection. Silicon photodiodes exhibit good responsivity, on the order of 0.1 to 1 A/W, over the entire visible and near-IR spectrum. Although the UV response in a standard *p–n* photodiode is significantly lower than the peak response in the near-IR region, photodiodes are manufactured that exhibit enhanced blue and UV response. Due to the broad spectral response, if visible blind operation is desired, the incident light must be spectrally filtered to remove the visible and near-IR wavelengths. The typical spectral response for a Si *p–n* junction is shown in Fig. 1, exhibiting a peak at ~900 nm and a broad long-wavelength cutoff extending beyond 1100 nm, due to the indirect nature of the Si band gap. The response in the UV region is essentially zero for wavelengths shorter than ~300 nm. The construction of a typical silicon *p–n* junction photodiode is shown in Fig. 2. In this example, a single-crystal, high-purity, *n*-type silicon substrate is doped with a material, such as boron, to form a thin *p* layer on one surface. The *p* layer may be formed by thermal diffusion or ion implantation of the boron to depths of ~1 μm or less. The interface between the *p*-doped Si and the *n*-doped Si com-

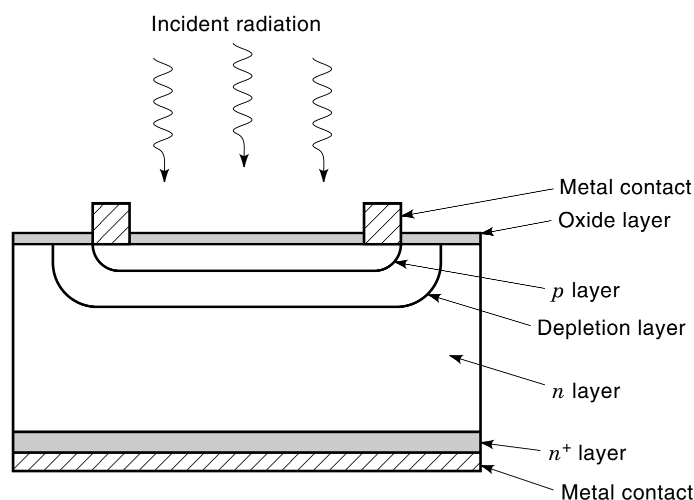

Figure 2. Schematic of a typical *p–n* junction Si photodiode.

prises the p–n junction. P–n junction photodiodes operate by the absorption of light in the bulk of the semiconductor. In the figure, light is incident on the surface with the diffused p layer. Since Si has a high absorption coefficient, particularly for blue and UV wavelengths, the p layer at this surface must be thin enough to permit good interaction of the light with the bulk semiconductor near the p–n junction. The absorption of light creates electron-hole pairs that are subsequently separated by the electric field of the p–n junction. The electrons move toward the n layer and holes move toward the p layer. The notation p^+ and n^+ designate heavily doped p and n layers, respectively. Such layers have high conductivity and are used to ensure good electrical contact between the semiconductor and the metal conductor. The open-circuit voltage generated by the photoinduced charge is extremely linear with respect to the intensity of the light. If the anode and cathode of the photodiode are connected across a resistive load, this internal charge migration is measured externally as a photocurrent that is similarly found to be linear with the light intensity over a wide dynamic range. The operation of p–n junction photodiodes in this zero-bias photovoltaic mode is used for applications requiring the greatest sensitivity; however, increased speed and linearity can be attained by applying a reverse bias (the photocurrent remains the same). The reverse bias reduces the capacitance of the device, thereby decreasing the RC time constant and improving the temporal response of the photodiode. However, the bias also increases the dark current, resulting in an overall reduction in sensitivity. There is therefore a trade-off between sensitivity and speed in an ordinary p–n junction photodiode.

For the specific application of ultraviolet light detection the p–n junction photodiode must be optimized in a number of ways to enhance the quantum efficiency of the device to UV light and to avoid the loss of carriers to nonradiative recombination processes, particularly at surfaces and interfaces. The quantum efficiency is defined as the number of electron-hole pairs per incident photon that are generated and which are subsequently separated by the electric field of the p–n junction before recombination occurs. High quantum efficiency requires that the incident light be able to penetrate into the bulk of the semiconductor material to generate carriers near the junction. Due to the high absorptivity of Si the penetration depth of light is very small and standard Si photodiodes are fabricated with a relatively thin layer, $\sim$1 μm or less, of doped material on the surface upon which the light is incident. Figure 3 shows the absorption coefficient of Si as a function of wavelength (4). For the wavelength range from 10 nm to 400 nm the absorption length is everywhere less than 100 nm and reaches a minimum value of 3 nm at a wavelength of $\sim$300 nm. Thus, the quantum efficiency in the UV region is reduced, even for submicrometer-thick layers, because of the exceptionally strong absorptivity at these wavelengths. Obviously, the thickness of the doped layer must be kept as thin as possible to enhance the UV response. It follows that the shallow p–n junction lies very near the surface of the photodiode. Because of the high doping levels typically used and the close proximity of the charge carriers with the surface, nonradiative recombination of carriers can cause a significant loss of quantum efficiency. In order to minimize the probability of carrier recombination the surface can be passivated with a thin coating of a material such as silicon dioxide. This oxide coating is also intended to protect the photodiode surface from moisture, chemicals, and scratches and serves as an antireflection coating to reduce incident light losses. Control of the thickness and quality of the oxide coating is important for optimizing the UV response. The quality of this coating and the nature of the interaction at the interface between the coating and the semiconductor are largely responsible for aging effects that have been observed in the UV response of Si photodiodes. This has been a significant problem for Si photodiodes, with extended UV exposure, even at low power, capable of causing substantial degradation in the response (5–7). The quantum efficiency of a Si photodiode decreased (5) from an initial value of 27% to less than 8% when illuminated with 10^{10} photons/(s · mm^2) at 124 eV for less than 30 min. UV-enhanced Si photodiodes having superior stability as well as high quantum efficiency (8,9) were manufactured by diffusing arsenic or phosphorus in a thin, highly doped layer on p-type Si. The superior characteristics of the photodiodes were attributed to the n on p construction and careful control of the quality and thickness of the oxide coating. These photodiodes have been further improved more recently (10,11) by nitriding the oxide layer to yield an oxynitride layer that possesses significantly improved radiation hardness and resistance to moisture. Because of the ruggedness of the 60 Å thick oxynitride layer and the virtual absence of nonradiative recombination at the oxynitride/silicon interface, the photodiodes possess high quantum efficiency with exceptional long-term stability. The same photodiodes, with the responsivity calibrated as a function of wavelength in the vacuum UV, are available from the National Institute of Standards and Technology (NIST) as transfer standard detectors. A schematic of the photodiode is shown in Fig. 4 and the wavelength dependence of the responsivity is shown in Fig. 5.

To summarize, UV-enhanced Si photodiodes are widely used for UV photodetection because they can be manufactured using well-established wafer-scale processing methods and they are relatively inexpensive. They are commercially available from a number of manufacturers (12). However, their response in the UV region is much smaller than their response in the visible and near-IR regions so that if solar blind operation is required, then optical filters, such as colored glass filters and dielectric coated band-pass filters, must be used with the photodiode to block the longer wavelengths. In addition, the quantum efficiency in the UV region can vary significantly with wavelength due to the rapidly varying absorption coefficient of Si at UV wavelengths, the related problem of nonradiative recombination losses close to the surface

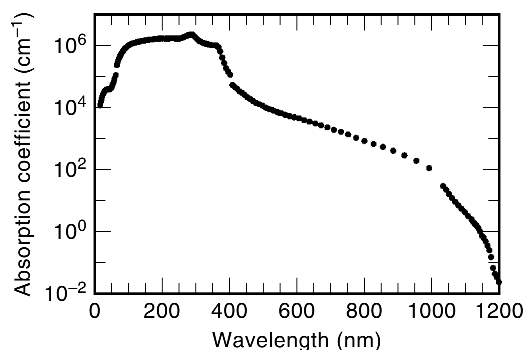

Figure 3. Absorption coefficient of Si as a function of wavelength for UV, visible, and near-infrared wavelengths.

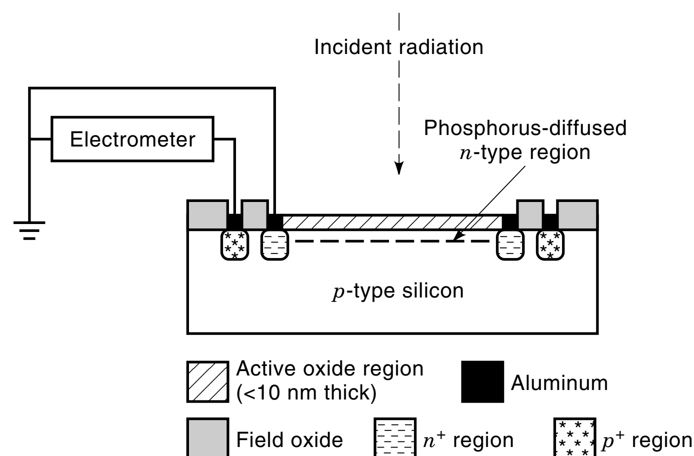

Figure 4. Schematic of a state-of-the-art UV-enhanced Si photodiode. (Courtesy of the Physics Laboratory, National Institute of Standards and Technology.)

due to the short absorption lengths and because of the finite probability of creating more than one electron-hole pair per UV photon. Finally, when choosing a Si photodiode, the stability of the UV response with age and with accumulated UV exposure is an important consideration.

GaP and GaAsP Schottky Photodiodes

The second semiconductor photodiode architecture that is well suited for UV photodetection applications is the Schottky photodiode. In the diffusion-type p–n junction photodiode, discussed above, the depletion layer is formed between the p-doped and n-doped layers of the semiconductor while in a Schottky photodiode the depletion layer is formed at the interface between the semiconductor and a thin layer of metal, such as gold or platinum. Since the photosensitive region is located nearer to the surface, the Schottky barrier photodiode is capable of superior short-wavelength detection than the p–n junction if the material is highly absorbing. A schematic of a Schottky barrier photodiode is shown in Fig. 6. In this figure a thin layer of gold is deposited on an n-type substrate. The gold layer is thin enough, typically about 10 nm, to permit ultraviolet light to penetrate into the semiconductor layer. Photogenerated electron-hole pairs are collected in the

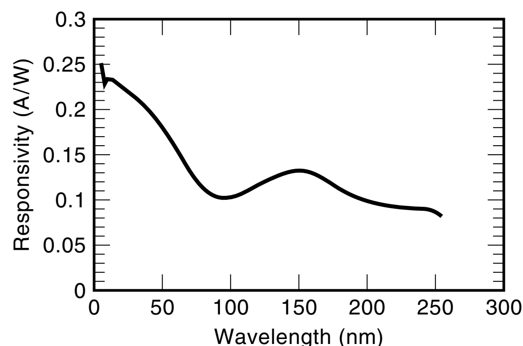

Figure 5. Spectral response of UV-enhanced Si photodiode. (Courtesy of the Physics Laboratory, National Institute of Standards and Technology.)

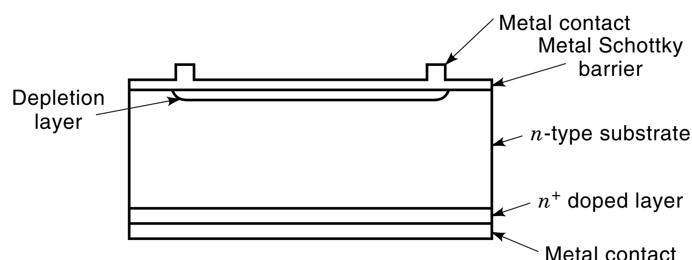

Figure 6. Schematic of a typical Schottky barrier photodiode.

depletion layer near the metal/semiconductor interface and are separated by the depletion layer field, giving rise to an external photocurrent, just as in the case for the p–n junction photodiode. Schottky barrier photodiodes are relatively simple to fabricate compared to diffused junction photodiodes, since the junction is formed by the deposition of a single thin layer of metal on the semiconductor surface. The spectral response of the resulting photodiode depends on the response of the semiconductor. Ultraviolet sensitive Schottky photodiodes have been fabricated using Si, however, it was found that the quantum efficiency degraded with exposure in a manner essentially identical to that observed for p–n junction Si photodiodes (5). Commercially available (13) alternatives to Si photodiodes include GaP and GaAsP Schottky-type photodiodes. These photodiodes are manufactured using a thin layer of gold on an n-type semiconductor substrate. The stability of GaP and GaAsP Schottky photodiodes is superior to that of Si photodiodes, and it has been shown that (5) the quantum efficiencies of the GaP and GaAsP Schottky photodiodes remain constant over time with UV irradiation. Both GaP and GaAsP photodiodes have good sensitivity throughout the entire UV region and are more resistant to radiation damage than Si photodiodes. The spectral responsivity of a GaP Schottky photodiode is shown in Fig. 7. Since GaP and GaAsP are wider-band-gap materials than Si, they offer greater selectivity in the wavelength response. GaAsP photodiodes exhibit a peak response at ~600 nm and a relatively sharp cutoff at ~680 nm, while the peak of the response for GaP is

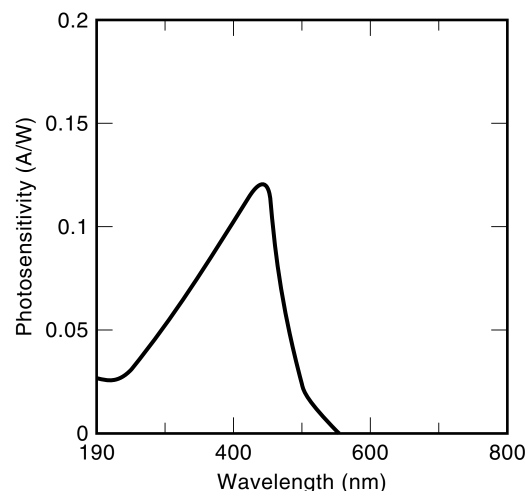

Figure 7. Spectral response of a GaP Schottky barrier photodiode. (Courtesy of Hamamatsu Corporation.)

~450 nm, with a cutoff at ~550 nm. Although the quantum efficiencies of the GaP and GaAsP photodiodes are lower than the quantum efficiency for Si photodiodes, the spectral responsivities of GaP and GaAsP in the ultraviolet region are smoothly varying functions of wavelength. This is in contrast to the responsivity of Si, which exhibits abrupt excursions throughout the UV region due to multiple photon ionization. The rise time of the temporal response of the GaP and GaAsP Schottky photodiodes is significantly longer than that of a p–n junction photodiode, ranging from 5 μs to 50 μs for photodiodes having active areas that range from 1 mm × 1 mm to 10 mm × 10 mm, respectively. This is because the capacitance of the Schottky barrier photodiodes are significantly larger as a result of the extremely thin depletion layer. The surface barrier structure also leads to higher dark currents in the GaP and GaAsP photodiodes compared to Si photodiodes.

Wide-Band-Gap Materials

The semiconductor photodetectors discussed thus far have differed with respect to the substrate material and the nature of the barrier that separates the photogenerated carriers. In all cases the responsivity of the photodiode was greater in the visible and near-IR regions than in the ultraviolet region. For many applications it is desirable for a photodetector to exhibit high responsivity to ultraviolet wavelengths and negligible responsivity to visible and near-IR wavelengths (greater than 400 nm). This kind of operation is often referred to as visible-blind detection. Solar-blind detection is a class of visible-blind operation having even more stringent wavelength requirements, exhibiting high responsivity to only those wavelengths less than 290 nm. Solar blind operation is impossible to achieve using Si photodetectors without the use of filters such as UV-transmitting–visible-blocking colored-glass filters usually in combination with dielectric-coated band-pass filters. The use of these spectral filtering techniques, however, imposes certain restrictions on the operation of the resulting photodiode-filter assembly. Most band-pass filters are made by combining dielectric stack interference filters with additional colored-glass or metal-film blocking filters. While these band-pass filters offer some flexibility in the specification of the center wavelength (or edge wavelength) and the width of the band, the overall transmission off-band cannot be reduced to a value less than 10^{-4} without seriously degrading the transmission within the band. In addition, the transmission characteristics of interference-type filters are extremely angle dependent and often can accept only a small field of view. Colored-glass filters by themselves are not capable of rejecting both visible and near-IR wavelengths and their transmission in the ultraviolet degrades as the glass ages. For these reasons the field of solar-blind photodetection is an active area of research and development. In particular, the development of photodetectors manufactured using wide-band-gap materials (direct and indirect) offers the potential for developing true solar-blind detectors that have negligible visible and near-IR response. In addition to superior spectral selectivity, wide-band-gap materials exhibit superior physical properties compared to Si, such as higher thermal conductivity, better radiation hardness and durability, and greater resistance to dielectric breakdown. These properties permit the use of wide-band-gap photodetectors in environmentally demanding applications that require resistance, for example, to high temperature, high voltage, or high incident power. The wide-band-gap materials that have received the greatest scrutiny for UV photodetector applications are silicon carbide (SiC), III–V nitrides, such as gallium nitride (GaN), and diamond. Silicon carbide and the III–V nitrides are discussed later. Diamond is potentially an ideal solar-blind detector because of its wide band gap (5.5 eV), low electrical conductivity, and chemical inertness. Natural diamond has been used previously, with significant restrictions and limitations, as a photoconductive detector for ultraviolet and ionizing radiation. More recently, the growth of polycrystalline diamond films by chemical vapor deposition methods has raised significant anticipation for the development of diamond-based UV detectors. However, high-quality undoped and n-doped diamond films have proven difficult to prepare. Structural defects in the polycrystalline films are responsible for defect states that can generate an unwanted subgap photoresponse. Diamond UV detectors will not be discussed in detail and the interested reader is referred to the literature (14–17) for the latest developments in diamond materials research and diamond UV detector device development.

Silicon Carbide. Hexagonal, crystalline silicon carbide (6H-SiC) is a wide-band-gap (2.9 eV at 300 K) semiconductor that absorbs UV light, but is essentially transparent to IR and visible light. The strength of the Si–C bond (bond energy ~5 eV) provides the material with superior resistance to high temperatures, chemicals, and mechanical shock. The width of the band gap results in low dark currents, even at elevated temperatures, thereby permitting sensitive photodetection under widely varying environmental conditions. While the device fabrication techniques for SiC materials are not as mature as those for Si fabrication, recent progress has yielded good-quality, bulk 6H–SiC single crystals that are used as substrates for the subsequent deposition of epitaxially grown p-type and n-type layers (18). Both p–n junction and Schottky barrier SiC photodiodes have been reported (19–23). High-quality p–n junction SiC photodiodes are commercially available as a chip (18,21) or packaged within a fixture (24,25). A schematic of the photodiode is shown in Fig. 8. A wafer of p-type 6H–SiC is used as the substrate and an epitaxial junction is fabricated by first growing an aluminum doped p-type layer followed by a nitrogen-doped n-type layer. The responsivity of the photodiode depends on the degree of doping and the thickness of these layers. A mesa is patterned and etched

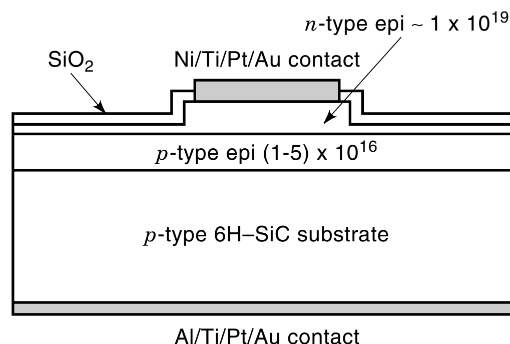

Figure 8. Schematic of a typical 6H–SiC photodiode. [Courtesy of Cree Research, Inc. Reprinted with permission from *Phys. Status Solidi A,* **162**, 481, 1997. Copyright 1997 Wiley-VCH Verlag.]

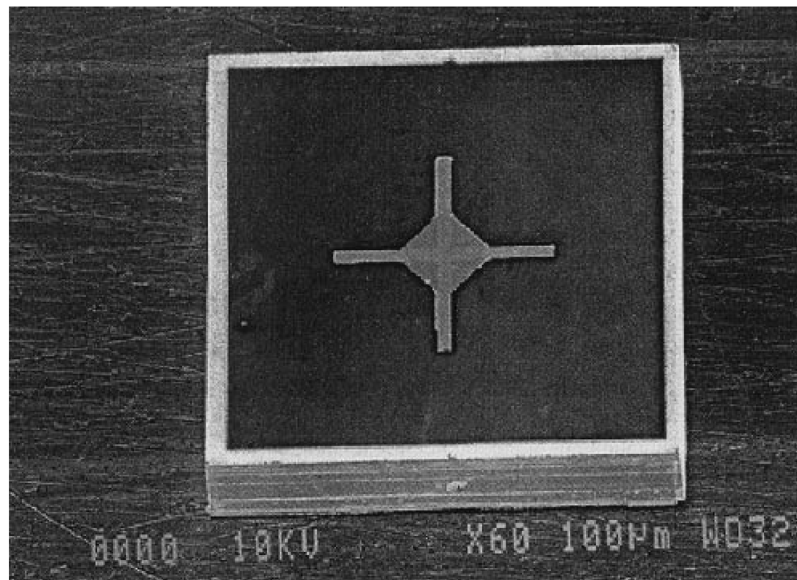

Figure 9. SEM micrograph of a typical 6H–SiC photodiode. [Courtesy of Cree Research, Inc. Reprinted with permission from *Phys. Status Solidi A,* **162**, 481, 1997. Copyright 1997 Wiley-VCH Verlag.]

using reactive ion etching. The typical size of the mesa varies from 0.09 mm^2 to 9 mm^2. A 50-nm-thick silicon dioxide layer is used to passivate the surface. A cross-shaped Al contact covers less than 2% of the area of the mesa. A scanning electron microscope (SEM) micrograph of the SiC photodiode is shown in Fig. 9. Although the absorption length of UV light in SiC is greater than it is in Si, the responsivity of the SiC photodiode is improved by limiting the thickness of the n^+ layer to ~0.1 μm. The responsivity and quantum efficiency of the SiC photodiode are shown in Fig. 10 as a function of wavelength at several temperatures. The spectral response curves are smoothly varying functions of UV wavelength from 200 nm to 400 nm, exhibiting peaks at ~275 nm to ~300 nm, with corresponding maximum quantum efficiencies ranging from 80% to 100%. The response curves shift to lower energy with temperature due to the shift in the band gap with temperature from ~3.03 eV at 223 K to ~2.88 eV at 623 K. The dark current, as expected, is quite low in these photodiodes. Figure 11 shows the reverse-bias dark-current density versus voltage as a function of temperature for a SiC photodiode having an active area of 0.04 cm^2. At a typical operating bias of -1.0 V, the dark current at 473 K is ~10^{-11} A/cm^2. Extrapolated to room temperature, this corresponds to an extremely low dark-current density of ~2×10^{-17} A/cm^2 at a reverse bias of -1.0 V. Comparing the performance of the SiC photodiode to a UV-enhanced Si photodiode, we find the SiC possesses a number of advantages. First, the response of SiC peaks near 300 nm and falls dramatically after 400 nm, while

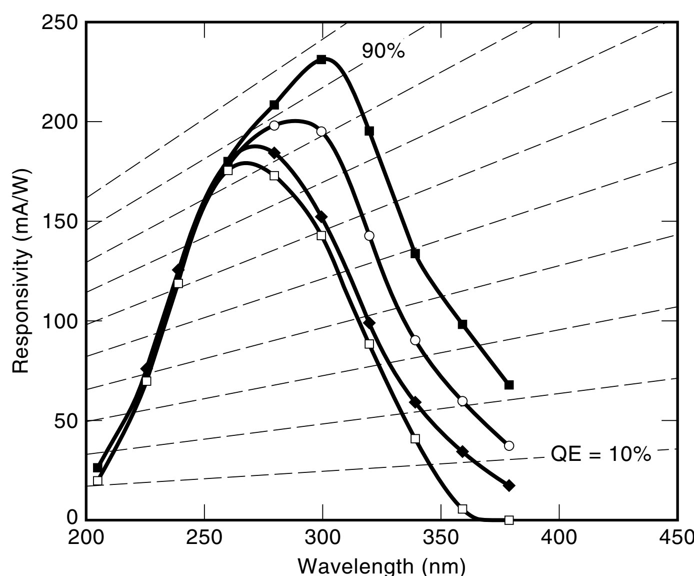

Figure 10. Spectral response of a typical 6H–SiC photodiode at several temperatures. Open squares: 223 K; diamonds: 300 K; circles: 498 K; and solid squares: 623 K. The peak quantum efficiency (QE) varies from 82% to 96% as a function of temperature. [Courtesy of Cree Research, Inc. Reprinted with permission from *Phys. Status Solidi A,* **162**, 481, 1997. Copyright 1997 Wiley-VCH Verlag.]

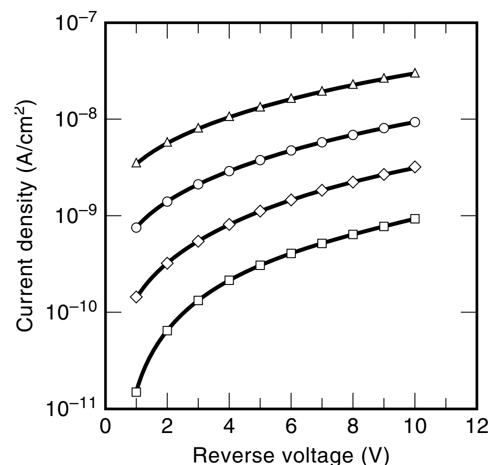

Figure 11. Dark current density of a typical 6H–SiC photodiode as a function of reverse-bias voltage at several temperatures. Squares: 473 K; diamonds: 523 K; circles: 573 K; and triangles: 623 K. [Courtesy of Cree Research, Inc. Reprinted with permission from *Phys. Status Solidi A,* **162**, 481, 1997. Copyright 1997 Wiley-VCH Verlag.]

that of Si peaks near 900 nm and extends to ~1200 nm. Therefore, for many applications, blocking filters are not required to eliminate unwanted visible and near-IR wavelengths in SiC while they are critical in Si. The responsivity of the SiC photodiodes is ~0.2 A/W to ~0.25 A/W near 300 nm, about the same or even greater than that of UV-enhanced Si photodiodes at the same wavelength. SiC photodiodes can operate with low noise at significantly higher temperatures than Si photodiodes and provide greater long-term radiation resistance and stability than do Si photodiodes. (The ability to operate at high temperatures depends also on the limitations of the package that houses the semiconductor material and provides for electrical connections.) Recently, a thin-film photodetector utilizing amorphous SiC was reported (26). The photodetector was a *p–i–n* structure made of hydrogenated amorphous Si and SiC in a sandwich configuration on a glass substrate. A schematic of the photodetector is shown in Fig. 12. Photogeneration of carriers due to UV light absorption occurred only in the α-SiC : H *p* layer, so the device exhibited good wavelength selectivity in rejecting visible and near-IR light. The primary advantage of this technology is the potential for fabricating low-cost, large-area arrays of photodiodes on a wide variety of substrates.

III-V Nitrides. Wide-band-gap materials that have been intensively studied in recent years are the III–V nitrides, including, in particular, gallium nitride (GaN), aluminum nitride (AlN), and alloys of the two, $Al_xGa_{1-x}N$ ($0 \leq x \leq 1$). GaN and AlN are direct-gap materials with band gaps of 3.4 eV and 6.2 eV, respectively, at 300 K. The band gaps of AlGaN alloys are also direct and can cover the range from 3.4 eV to 6.2 eV continuously, depending on the relative concentrations of Al and Ga. Therefore, optical devices developed using these materials will have cutoff wavelengths ranging from 365 nm to 200 nm. Devices of interest include light-emitting diodes and laser diodes in addition to UV photodetectors. The electronic properties of GaN provide for superior solar-blind wavelength selectivity, high dielectric breakdown thresholds, high thermal conductivity, and excellent mechanical hardness. These features offer the potential for operation of solar-blind GaN UV photodetectors without using long-wavelength

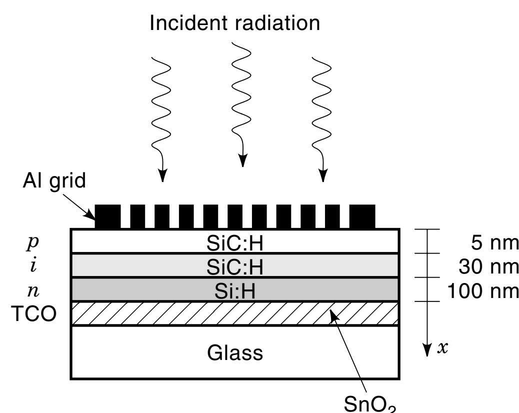

Figure 12. Schematic of thin film SiC photodetector fabricated using amorphous SiC and amorphous Si on a glass substrate. TCO = transparent conductive oxide film. [Reprinted with permission from *IEEE Trans. Electron Devices,* **43**, 1351, 1996. © 1996 IEEE.]

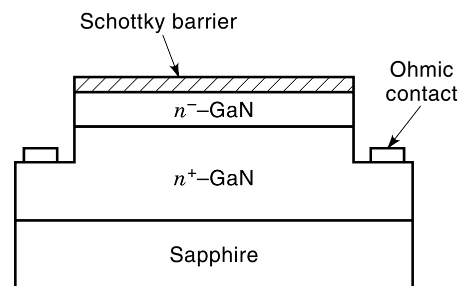

Figure 13. Schematic of vertical geometry, transparent GaN Schottky barrier photodiode. [Courtesy of APA Optics, Inc. Reprinted with permission from *Appl. Phys. Lett.,* **70**, 2277, 1997. Copyright 1997 American Institute of Physics.]

cutoff filters. Also, these photodiodes may be operated under extreme environmental conditions such as high temperature and high humidity. The realization of such devices has been impeded because of the difficulty of fabricating high-quality intrinsic and *p*-doped materials. For this reason GaN manufacturing technology is still considered an art and is much less mature than that for Si or SiC. Since there is no suitable material that will lattice match it, GaN films are usually grown at high temperature on sapphire substrates. Metal-organic chemical vapor deposition and molecular beam epitaxy techniques can yield high-quality films on sapphire substrates. These have been used to demonstrate exceptionally good solar-blind UV photodetection. The first demonstration of UV photodetection using single-crystal GaN films was reported by Khan and coworkers (27). A photoconductive detector using interdigitated electrodes (due to the extremely high resistivity of GaN) exhibited excellent responsivity for wavelengths shorter than 365 nm and very little responsivity for wavelengths longer than 365 nm, with an extremely sharp cutoff due to the direct gap. This device had a very high photoconductive gain (responsivity >1000 A/W), but had a long response time (order of ms). It has been found that both the responsivity and temporal response of photoconductive GaN detectors are functions of the incident power (28). This is the result of a competition between distinct recombination processes that involve deep traps within the GaN. More recently, a vertical geometry, transparent GaN Schottky barrier detector that uses front illumination has been described (29). A schematic of the detector is shown in Fig. 13. The vertical geometry of this detector resulted in efficient photocarrier collection and in a substantially improved response time (118 ns for a 50 Ω load). The spectral response of the Schottky photodiode for a −5 V bias is shown in Fig. 14. The response is relatively constant, ~0.15 A/W to 0.18 A/W, from 250 nm to the band edge at 365 nm. Although GaN photodetectors are available commercially (30) the fabrication of GaN epitaxial films and the development of photovoltaic and photoconductive detectors is still a topic of intense current research (31–36).

PHOTOEMISSIVE ULTRAVIOLET PHOTODETECTORS

In a semiconductor photodetector ultraviolet light is absorbed within the semiconductor, producing electron-hole pairs that are then separated by an electric field, giving rise to the pho-

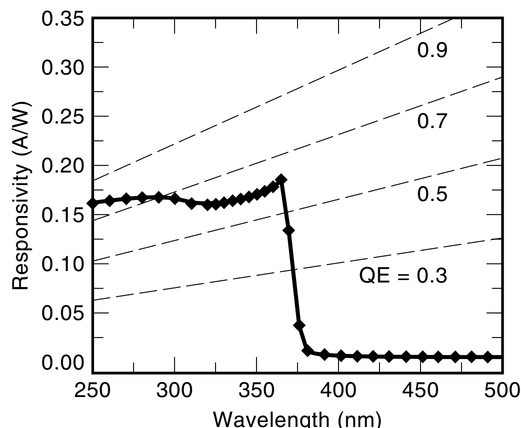

Figure 14. Spectral response of GaN Schottky barrier photodiode. [Courtesy of APA Optics, Inc. Reprinted with permission from *Appl. Phys. Lett.,* **70**, 2277, 1997. Copyright 1997 American Institute of Physics.]

toconductive and photovoltaic effects. In a photoemissive photodetector, however, ultraviolet light ejects photoelectrons from the surface of a photocathode, generating a photoelectron current when the photoelectrons are collected by an anode at a positive bias with respect to the cathode. The photoelectron current is proportional to the intensity of the incident ultraviolet light. The spectral response of the detector depends largely on the work function of the photocathode material. Vacuum photodiodes are relatively simple photoemissive detectors that can have subnanosecond time resolution. They are well suited for applications that require the measurement of relatively intense, fast UV light signals (37). A schematic of a windowless aluminum oxide photoemissive photodiode (38) is shown in Fig. 15. The photocathode is manufactured by evaporating a thin film of aluminum onto a quartz disk and oxidizing the surface to yield a thin layer (~15 nm) of aluminum oxide. The anode is a stainless-steel ring that is assembled with the photocathode in a Teflon body. The response of this photodetector is quite solar blind, exhibiting a peak at ~70 nm and falling to essentially zero beyond 150 nm. The response at the peak is 0.16 electrons/photon, reflecting the fact that while these photodetectors can have high quantum efficiency there is no internal gain.

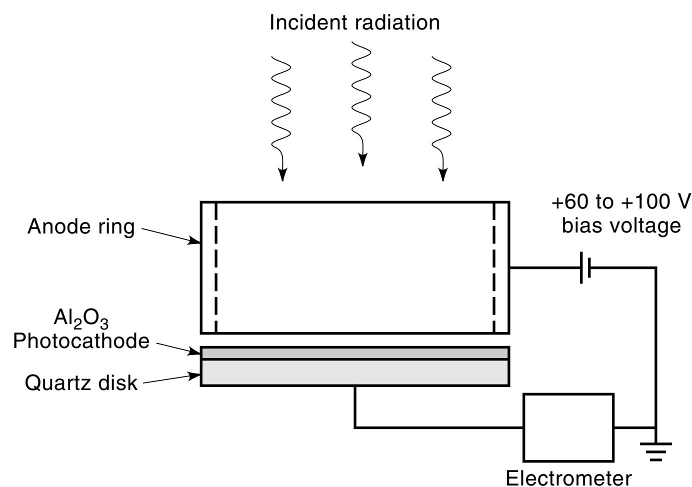

Figure 15. Schematic of windowless aluminum oxide photoemissive photodiode. [Courtesy of the Physics Laboratory, National Institute of Standards and Technology.]

Photomultiplier Tubes

The primary photoelectrons produced by incident photons at the photocathode can be multiplied to provide a photoemissive detector with high gain. Photomultiplier tubes (PMTs) are photoemissive detectors with very high gain that provide the most sensitive method for measuring low light levels (39). The principle elements of a PMT are shown schematically in Fig. 16 and include a photocathode, an electron multiplier, and an anode, all of which are contained in a vacuum envelope. A photon impinges upon the photocathode of a PMT, causing a photoelectron to be ejected and accelerated toward the electron multiplier or dynode chain. The initial photoelectron impacts the surface of the first dynode, causing the emission of several secondary electrons, which in turn cascade through the dynode chain resulting in gains of 10^5 to 10^6 secondary electrons per photoelectron. The resulting electron current is detected at the anode. Depending on the rate at which the incident photons arrive, the output of the PMT may appear as short bursts of voltage pulses for low light levels or as a dc current for higher light levels. The most sensitive method for the measurement of low light levels ($N < 10^8$ photons/s) is single photon counting. This method counts the number of photoelectron-generated pulses that arrive at the anode during a preselected time interval. A voltage discriminator is used to discriminate between voltage pulses that originate from the photocathode (signal) and voltage pulses that originate from within the dynode chain (noise). For higher light levels, current measurement methods are used. There are a variety of types of electron multipliers that are used in PMTs including several types of dynode chains, wire mesh dynodes, and microchannel plates. Specific dynode structures are chosen for particular applications, for example, a linear focused dynode chain provides fast response times and is particularly useful for pulsed measurements, while a box and grid type dynode chain provides excellent photon collection efficiency (40). Wire mesh and microchannel plate electron multiplier structures may be used for position-sensitive detection applications. These types of electron multipliers are particularly insensitive to external magnetic fields, and can be used in environments that are not suitable for most other PMTs. For the specific application of UV light detection, the wavelength response of a PMT is dependent on a number of

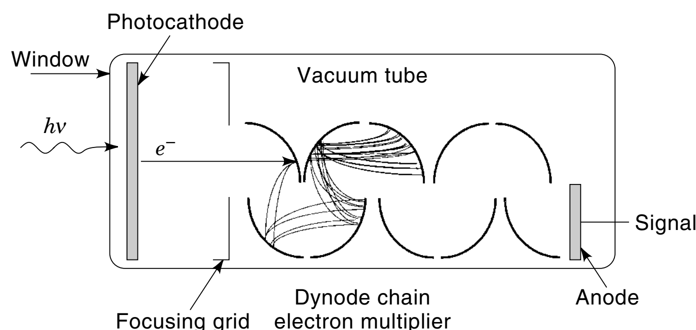

Figure 16. Schematic of a typical photomultiplier tube.

factors including the window material used to seal the vacuum tube and the composition of the photocathode material. Windows composed of MgF_2 provide transmission down to 105 nm. Other UV-transmitting window materials include LiF, sapphire, and synthetic fused silica, with minimum transmission wavelengths of 115 nm, 145 nm, and 160 nm, respectively. Commercially available solar-blind, UV-sensitive PMTs utilize photocathode materials such as CsI, CsTe, KBr, and RbTe. The spectral response for a photomultiplier manufactured using a CsI photocathode and a magnesium fluoride window (13) extends from 115 nm to 195 nm, with the peak of the response occurring at ~120 nm. The spectral response for a photomultiplier manufactured using a CsTe photocathode and a synthetic silica window (13) extends from 160 nm to 320 nm, with the peak of the response occurring at ~200 nm. The short-wavelength cutoff for these photomultiplier tubes is determined by the absorption coefficient of the window material, while the long-wavelength limit is determined by the work function of the photocathode material. These UV-sensitive photocathodes are particularly useful for solar-blind detection applications as they are practically unresponsive to visible light wavelengths and can often be used without filters to block background light. Solar-blind PMTs are commercially available from a number of suppliers (12). Other photocathode materials are available with good UV sensitivity, such as bi-alkali, S-20, and S-11 photocathodes, but these are not visible-blind photocathodes, and appropriate wavelength discrimination using filters or monochromators is required to exclude visible light. Generally, although PMTs do not have the high quantum yield of semiconductor detectors, their large gain and low noise are necessary for very-low-light-level applications. Traditionally, the expense, mechanical fragility, susceptibility to magnetic fields, and high-voltage power requirements of PMTs have been important considerations in determining their use. Advances in PMT technology are challenging these traditional considerations as miniaturized PMTs, and PMT modules provide exceptional performance in small, rugged packages (13).

Gas-Filled Phototubes

The gas-filled phototube is another type of photoemissive photodetector that is used for solar-blind ultraviolet light detection applications. In these detectors a dc gas discharge is maintained by a small discharge current from a metal photocathode to a wire anode. When the gas discharge is illuminated with very low levels of ultraviolet light, gas breakdown occurs leading to an increase in the discharge current. The bias current is set near the breakdown condition and the response is nonlinear, exhibiting saturation at relatively low (nanowatt) power. Commercially available gas-filled phototubes (41) have a solar-blind spectral response (185 nm to 260 nm) and are used in flame detectors and fire alarms. Improved gas-filled phototubes have been described more recently (42) that operate without gas breakdown and are significantly more sensitive than the gas-discharge tubes. These phototubes operate in the prebreakdown regime and detect light by an excited-state photoionization mechanism rather than glow discharge. The responsivity in the ultraviolet region is quite high, 6 A/W at 200 nm using molybdenum electrodes and argon gas, due to the internal gain. The response of these phototubes ranges from 190 nm to 270 nm.

BIBLIOGRAPHY

1. P. R. Norton, Photodetectors, in M.Bass (ed.), *Handbook of Optics, vol. I, Fundamentals, Techniques and Design,* 2nd ed., New York: McGraw-Hill, 1995.
2. G. R. Carruthers, Ultraviolet and x-ray detectors, in R. W. Waynant and M. N. Ediger (eds.), *Electro-Optics Handbook,* New York: McGraw-Hill, 1994.
3. M. Razeghi and A. Rogalski, Semiconductor ultraviolet detectors, *J. Appl. Phys.,* **79**: 7433–7473, 1996.
4. D. E. Aspnes, Optical functions of intrisic Si: Table of refractive index, extinction coefficient and absorption coefficient vs energy (0 to 400 eV), in *Properties of Silicon, EMIS Datareviews Series No. 4,* London: Institution of Electrical Engineers, 1988.
5. M. Krumrey et al., Schottky type photodiodes as detectors in the VUV and soft x-ray range, *Appl. Opt.,* **27**: 4336–4341, 1988.
6. N. M. Durant and N. P. Fox, Evaluation of solid-state detectors for ultraviolet radiometric applications, *Metrologia,* **32**: 505–508, 1995/96.
7. E. Tegeler and M. Krumrey, Stability of semiconductor photodiodes as VUV detectors, *Nucl. Instrum. Meth. Phys. Res. A,* **282**: 701–705, 1989.
8. R. Korde and J. Geist, Stable, high quantum efficiency, UV-enhanced silicon photodiodes by arsenic diffusion, *Solid State Electron.,* **30**: 89–92, 1987.
9. R. Korde and J. Geist, Quantum efficiency stability of silicon photodiodes, *Appl. Opt.,* **26**: 5284–5290, 1987.
10. R. Korde, J. S. Cable, and L. R. Canfield, One gigarad passivating nitrided oxides for 100% internal quantum efficiency silicon photodiodes, *IEEE Trans. Nucl. Sci.,* **40**: 1655–1659, 1993.
11. Product literature, International Radiation Detector, Inc. 2527 W. 237th St, Unit B, Torrance, CA 90505.
12. See the *Laser Focus World Buyers Guide* or *Photonics Buyers Guide* for comprehensive lists of vendors.
13. Hamamatsu Corp., 360 Foothill Road, Bridgewater, NJ 08807.
14. R. D. McKeag et al., Photoconductive properties of thin film diamond, *Diamond Relat. Mater.,* **6**: 374–380, 1997.
15. S. Salvatori et al., Photoelectrical characteristics of diamond UV detectors: Dependence on device design and quality, *Diamond Relat. Mater.,* **6**: 361–366, 1997.
16. E. Pace et al., Electrooptical properties of diamond thin films as UV photodetectors, *Nucl. Instrum. Meth. Phys. Res. A,* **387**: 255–258, 1997.
17. G. Popovici et al., Diamond ultraviolet photovoltaic cell obtained by lithium and boron doping, *J. Appl. Phys.,* **81**: 2429–2431, 1997.
18. Cree Research Inc., 2810 Meridian Parkway, Durham, NC, 27713.
19. D. M. Brown et al., Silicon carbide UV photodiodes, *IEEE Trans. Electron. Devices,* **40**: 325–333, 1993.
20. J. A. Edmond, H.-S. Kong, and C. H. Carter, Jr., Blue LEDs, UV photodiodes and high-temperature rectifiers in 6H-SiC, *Physica B,* **185**: 453–460, 1993.
21. J. Edmond et al., 6H-Silicon carbide light emitting diodes and UV photodiodes, *Phys. Status Solidi A,* **162**: 481–491, 1997.
22. C. Frojdh et al., UV-sensitive photodetectors based on metal-semiconductor contacts on 6H-SiC, *Phys. Scripta,* **T54**: 169–171, 1994.
23. R. G. Verenchikova et al., *Sov. Phys. Semicond.,* **26**: 565–568, 1992.
24. Boston Electronics Corporation, 72 Kent St., Brookline, MA 02146.
25. Laser Components, Inc., 70 W. Barham Ave., Santa Rosa, CA 95407.

26. D. Caputo et al., Solar-blind UV photodetectors for large area applications, *IEEE Trans. Electron. Devices,* **43**: 1351–1355, 1996.
27. M. A. Khan et al., High-responsivity photoconductive ultraviolet sensors based on insulating single-crystal GaN epilayers, *Appl. Phys. Lett.,* **60**: 2917–2919, 1992.
28. F. Binet et al., Mechanisms of recombination in GaN photodetectors, *Appl. Phys. Lett.,* **69**: 1202–1204, 1996.
29. Q. Chen et al., Schottky barrier detectors on GaN for visible-blind ultraviolet detection, *Appl. Phys. Lett.,* **70**: 2277–2279, 1997.
30. APA Optics, Inc., 2950 NE 84th Ln., Minneapolis, MN 55449.
31. J. M. Van Hove et al., Ultraviolet-sensitive, visible-blind GaN photodiodes fabricated by molecular beam epitaxy, *Appl. Phys. Lett.,* **70**: 2282–2284, 1997.
32. R. D. Vispute et al., Growth of epitaxial GaN films by pulsed laser deposition, *Appl. Phys. Lett.,* **71**: 102–104, 1997.
33. J. C. Carrano et al., Very low dark current metal-semiconductor-metal ultraviolet photodetectors fabricated on single-crystal GaN epitaxial layers, *Appl. Phys. Lett.,* **70**: 1992–1994, 1997.
34. D. Walker et al., $Al_xGa_{1-x}N$ ($0 \le x \le 1$) ultraviolet photodetectors grown on sapphire by metal-organic chemical-vapor deposition, *Appl. Phys. Lett.,* **70**: 949–951, 1997.
35. M. J. Malachowski and A. Rogalski, GaN ultraviolet photodiodes-photoresponse modelling, *J. Tech. Phys.,* **38**: 65–72, 1997.
36. M. Smith et al., Room temperature intrinsic optical transition in GaN epilayers: The band-to-band versus excitonic transitions, *Appl. Phys. Lett.,* **71**: 635–637, 1997.
37. C. V. S. Rao et al., Vacuum photodiode detectors for broadband vacuum ultraviolet detection in the Saha Institute of Nuclear Physics Tokamak, *Rev. Sci. Instrum.,* **68**: 1142–1148, 1997.
38. National Institute of Science and Technology, Physics Laboratory, Gaithersburg, MD.
39. G. F. Knoll, *Radiation Detection and Measurement,* 2nd ed., New York: Wiley, 1989.
40. E. J. Lerner, Photomultiplier tubes offer high-end sensitivity, *Laser Focus World,* 87–96, July 1996.
41. UV TRON flame detectors, Hamamatsu Corp., 360 Foothill Road, Bridgewater, NJ 08807.
42. M. Cohen and N. S. Kopeika, A near UV envelope detector in the prebreakdown regime based on photoionization of excited gas atoms, *Meas. Sci. Technol.,* **5**: 540–547, 1994.

ALAN L. HUSTON
BRIAN L. JUSTUS
Naval Research Laboratory

UNCERTAINTY MANAGEMENT. See BELIEF MAINTENANCE.

UNCERTAINTY MODELING. See DECISION THEORY.

UNCOOLED INFRARED DETECTOR ARRAYS. See INFRARED DETECTOR ARRAYS, UNCOOLED.